JOURNAL OF BACTERIOLOGY, Oct. 2006, p. 6924–6931 Vol. 188, No. 19
0021-9193/06/$08.00+0 doi:10.1128/JB.00831-06

Genomic Analysis of *Pseudomonas aeruginosa* Phages LKD16 and LKA1: Establishment of the ϕKMV Subgroup within the T7 Supergroup†

Pieter-Jan Ceyssens,[1] Rob Lavigne,[1] Wesley Mattheus,[1] Andrew Chibeu,[1] Kirsten Hertveldt,[1]* Jan Mast,[2] Johan Robben,[3] and Guido Volckaert[1]

Division of Gene Technology, Katholieke Universiteit Leuven, Kasteelpark Arenberg 21, Leuven B-3001, Belgium[1]*; Unit Electron Microscopy, Veterinary and Agrochemical Research Centre, Groeselenberg 99, Ukkel B-1180, Belgium*[2]*; and Biomedical Research Institute, Limburgs Universitair Centrum and School of Life Sciences, University Hasselt, Diepenbeek B-3590, Belgium*[3]

Received 12 June 2006/Accepted 20 July 2006

Lytic *Pseudomonas aeruginosa* phages LKD16 and LKA1 were locally isolated and morphologically classified as *Podoviridae*. While LKD16 adsorbs weakly to its host, LKA1 shows efficient adsorption ($k_a = 3.9 \times 10^{-9}$ ml min^{-1}). LKA1, however, displays a narrow host range on clinical *P. aeruginosa* strains compared to LKD16. Genome analysis of LKD16 (43,200 bp) and LKA1 (41,593 bp) revealed that both phages have linear double-stranded DNA genomes with direct terminal repeats of 428 and 298 bp and encode 54 and 56 genes, respectively. The majority of the predicted structural proteins were experimentally confirmed as part of the phage particle using mass spectrometry. Phage LKD16 is closely related to bacteriophage ϕKMV (83% overall DNA homology), allowing a more thoughtful gene annotation of both genomes. In contrast, LKA1 is more distantly related, lacking significant DNA homology and showing protein similarity to ϕKMV in 48% of its gene products. The early region of the LKA1 genome has diverged strongly from ϕKMV and LKD16, and intriguing differences in tail fiber genes of LKD16 and LKA1 likely reflect the observed discrepancy in infection-related properties. Nonetheless, general genome organization is clearly conserved among ϕKMV, LKD16, and LKA1. The three phages carry a single-subunit RNA polymerase gene adjacent to the structural genome region, a feature which distinguishes them from other members of the T7 supergroup. Therefore, we propose that ϕKMV represents an independent and widespread group of lytic *P. aeruginosa* phages within the T7 supergroup.

Two decades after the completion of the genome sequence of coliphage T7 (13), the T7 supergroup comprises 13 fully sequenced and highly virulent phages sharing common morphological, biological, and genomic characteristics. Extensive sequencing efforts have shown that the T7 supergroup can be subdivided further into distinct subgroups of phages that display more similarity to each other than to other members of the supergroup. Phages closely related to T7 (the T7 sensu stricto subgroup) include coliphages T3 (35) and K1F (46), *Yersinia* phages ϕA1122 (15) and ϕYe03-12 (36), and *Pseudomonas* phage gh-1 (23). One of the major distinctive characteristics of the T7 group was originally defined as the presence of a single-subunit phage RNA polymerase that binds phage-specific promoters. However, marine phages VpV262 and SIO1 share extensive homology with T7 but lack the phage RNA polymerase, probably constituting an ancient branch of the T7 supergroup (18). The discovery of a functional site-specific integrase in the genome of the marine T7-like phage P-SSP7 (M. B. Sullivan, personal communication) and of a T7-like prophage in the genome of *Pseudomonas putida* KT2440 (33) has led to a further breakdown of strict classification boundaries. Recently, an SP6 subgroup was proposed, containing the slightly more diverged *Salmonella* phage SP6 and coliphages K1-5 and K1E. The genome organization of these phages resembles that of T7, but numerous insertions and deletions throughout the genome are present, as shown by the presence of a P22-like spike protein (44). Despite clear vertical evolution among phages within the T7 supergroup (23), underlying mechanisms of horizontal evolution and genetic mosaicism are becoming evident within this group, as exemplified by the extensive homology between the T7-like prophage of *Pseudomonas putida* KT2440 and SP6 (12).

To date, the lytic *P. aeruginosa* phage ϕKMV is the only known T7-like phage coding for a phage RNA polymerase gene downstream of its DNA metabolism genes (26). Additional differences in genome organization compared to the sensu stricto T7 phages include the organization within the early region and subtle differences among the structural proteins (26). As in SP6, ϕKMV carries a functional lysin domain at the C terminus of the predicted internal protein gp36, while most members of the T7 group have this domain at the N terminus of the protein encoded by the downstream gene (25). The structural proteins were further analyzed, and 12 predicted proteins were recently confirmed as part of the ϕKMV phage particle (27). Lack of DNA homology to other phage genomes suggests that ϕKMV diverted early from the T7 group and developed an efficient virulent life cycle on *P. aeruginosa*.

Faced with worldwide bacterial resistance against numerous

* Corresponding author. Mailing address: Division of Gene Technology, Katholieke Universiteit Leuven, Kasteelpark Arenberg 21, Leuven B-3001, Belgium. Phone: 32 16 32 96 71. Fax: 32 16 32 19 65. E-mail: kirsten.hertveldt@biw.kuleuven.be.

† Supplemental material for this article may be found at http://jb.asm.org/.

antibiotics, there is a strong interest towards the antimicrobial potential and ecological diversity of lytic phages (48). In this context, bacteriophages LKD16 (Leuven, Kortrijk-Dutsel) and LKA1 (Leuven, Kasteelpark Arenberg) were recently isolated from Belgian environmental water samples. These phages were chosen based on their lytic properties towards environmental and clinical isolates of *P. aeruginosa*. We hereby present an in-depth characterization of both phages, elucidating their morphological and lytic characteristics, as well as their complete genome sequences and structural proteomes and their relationship to phage ϕKMV.

MATERIALS AND METHODS

Bacterial strains and growth media. *P. aeruginosa* PAO1 and 73 typed clinical *P. aeruginosa* strains were kindly provided by J. P. Pirnay (38). Bacterial strains were grown in standard Luria-Bertani medium. In procedures involving phage infection, 10 mM $MgSO_4$ was added to the medium.

Bacteriophage isolation, amplification, and purification. Phages LKA1 and LKD16 were isolated from 25-ml water samples which were filtered over a 0.45-μm membrane and incubated with exponentially growing *P. aeruginosa* PAO1 cells. After visible lysis of the bacteria, the culture was pelleted by centrifugation at 4°C and 8,000 × *g* for 20 min. Bacterial cell debris was removed by filtering (0.45 μm), and the presence of phage was verified by plating 100 μl of the filtrate using a standard soft agar overlay method (1). Single plaques were picked up and replated three times to ensure pure phage stocks. For phage propagation, 200 ml of a *P. aeruginosa* PAO1 culture (optical density at 600 nm of 0.4) was infected at a multiplicity of infection (MOI) of 0.1 and incubated until visible lysis. After addition of 5 ml chloroform and vigorous shaking, the culture was left overnight and cell debris was removed by centrifugation at 8,000 × *g*. Phages were precipitated with polyethylene glycol 8000 (8%, wt/vol)–1 M NaCl for 4 h, spun at 8,000 × *g* for 20 min, and resuspended in 15 ml phage buffer (10 mM Tris-HCl pH 7, 10 mM $MgSO_4$, 150 mM NaCl). This suspension was layered on a CsCl step gradient (1.33, 1.45, 1.50, and 1.70 g ml^{-1}) and centrifuged at 140,000 × *g* for 3 h. Both LKD16 and LKA1 were collected at ρ of 1.49 g ml^{-1} and dialyzed three times for 30 min against 300 volumes of phage buffer.

Electron microscopy. Purified bacteriophage particles were placed on carbon and pioloform-coated grids, negatively stained with 1% phosphotungstic acid, and visualized using an EM208S transmission electron microscope (FEI, Eindhoven, The Netherlands) operating at 80 kV as previously described (20).

Host range, growth curves, and adsorption assays. The host range of the phages was determined by standard spot tests (16) on both exponentially and stationary growing *P. aeruginosa* cells. The sensitivity of bacterial strains was confirmed by plaque assays and infection of liquid cultures at high MOI (10 to 100). One-step growth experiments were performed according to the method of Adams (1) with small modifications. Briefly, 5 min after infection of 1 ml *P. aeruginosa* (optical density at 600 nm of 0.5) at low MOI (0.005), the mixture was briefly spun (13,000 × *g*, 30 s) and a 10^{-5} dilution of the resuspended pellet was incubated at 37°C. Samples were taken from the broth at fixed intervals and immediately titrated. In adsorption experiments, the infection parameters of the growth curve experiment were maintained. Immediately after infection, 100-μl samples were taken at 30-s intervals and transferred to 850 μl LB supplemented with 50 μl $CHCl_3$. These mixtures were shaken for 10 min to lyse any remaining bacteria, followed by titration of the supernatant in order to determine the amount of nonadsorbed or reversibly adsorbed phage.

DNA isolation and sequencing. Phage DNA was isolated as described previously (43). Approximately 500 ng of phage DNA was partially digested with RsaI and NlaIV, and 1- to 2-kb DNA fragments were ligated into the SmaI site of the pUC18 vector for transformation with *Escherichia coli* XL1-Blue cells. Individual clones were used directly as template for sequencing as described by Ganguly et al. (14). After standard ethanol precipitation, the samples were separated and analyzed on an ABI 3130 capillary sequencing device (Applied Biosystems). Sequence assembly was performed with Sequencher 4.1 software (Genecodes). Gaps, direct repeats, and uncertainties in the sequence were determined by direct sequencing using phage-specific primers. To ensure quality of the data, every position was sequenced at least twice, and an average five- and sevenfold overall redundancy was obtained for LKD16 and LKA1, respectively.

In silico analysis. The genomes were scanned for potential open reading frames (ORFs) by using ORF Finder (http://www.ncbi.nlm.nih.gov/projects/gorf) and GeneMark.hmm (31). An extra iterative search with the ϕKMV sequence was performed for the annotation of LKD16 (see below). Translated ORF sequences were compared with known proteins using standard protein-protein BLASTP (2) and PSI-BLAST (3) programs against the nonredundant GenBank protein database. Prokaryotic promoters were predicted using the BDGP prediction program (39), and potential conserved intergenic motifs were scanned with MEME/MAST (4) and PHIRE (28) to identify phage regulatory elements. A search for transmembrane helices was done using the TMHMM algorithm (32). Direct, reverse, and palindromic repeat regions were identified with programs clustered by EMBOSS (40). Putative terminators were defined as palindromic sequences followed by a U-rich stretch and with a stable secondary structure (Δ*G* less than −10 kcal/mol), as calculated by MFold (55).

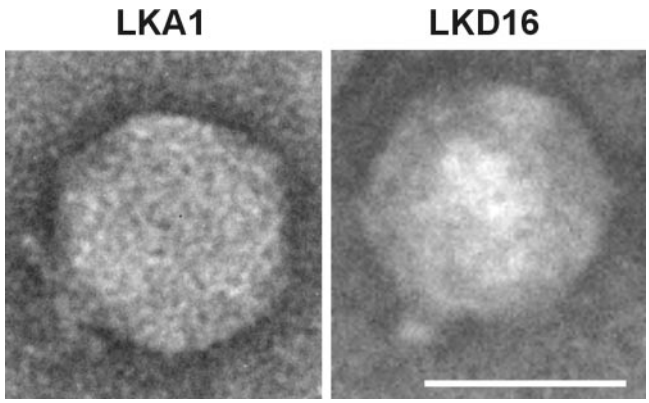

FIG. 1. Electron micrographs of negatively stained LKA1 and LKD16 particles. Bar, 50 nm.

Mass spectrometry. Peptide identification using electrospray ionization-tandem mass spectrometry (ESI-MS/MS) was performed essentially as described for ϕKMV (27). Briefly, phage particles were concentrated (Microcon; Millipore), reduced by β-mercaptoethanol, heat denatured (95°C, 5 min), and loaded on a standard 12% sodium dodecyl sulfate-polyacrylamide gel electrophoresis gel. The entire lane was cut into slices which were subjected to trypsin digestion (47). Peptides were separated by liquid chromatography with a linear 5 to 60% (vol/vol) acetonitrile gradient and subsequently identified by ESI-MS/MS in an *m/z* range of 300 to 1,500. All MS data were analyzed using Sequest (Thermofinnigan) considering minimal cross-correlation values of 1.8, 2.5, and 3.5 for single-, double-, and triple-charged peptide ions, respectively. All single- and double-peptide protein identifications were validated by reexamination with the de novo sequencing algorithm Lutefisk 1900 v.1.3.2 (27, 50).

Nucleotide sequence accession numbers. The GenBank accession numbers for the genomes of phages LKD16, LKA1, and ϕKMV are AM265638, AM265639, and AJ505558, respectively.

RESULTS

Phage characteristics. Bacteriophages LKD16 and LKA1 were isolated from local water sources and selected based on their ability to form clear plaques on *P. aeruginosa* PAO1. Electron microscopic imaging of purified phage particles revealed both phages as members of the *Podoviridae*, with a head diameter of approximately 60 nm and a stubby tail with a length of 8 to 10 nm (Fig. 1). The characteristic portal vertices are visible on the images of both phages, but possible tail fibers can only be distinguished in case of LKA1.

The infection process towards *P. aeruginosa* cells was investigated by standard adsorption and one-step growth assays and compared to that of ϕKMV. Under laboratory conditions, the infectivity properties of these phages differ considerably. Upon infection with LKD16, ϕKMV, and LKA1, host cells lyse after 25, 35, and 40 min, respectively, releasing approximately 120, 55, and 225 new phage particles per cell. Adsorption assays show that LKA1 particles efficiently absorb to *P. aeruginosa* cells ($k_a = 3.9 \times 10^{-9}$ ml min^{-1}), resulting in a 3-log reduction

in nonadsorbed phage particles 4 min after infection. This is in sharp contrast with LKD16 and ϕKMV, which both failed to produce a clear adsorption curve, showing only minor adsorption to host cells (20 to 30% at an MOI of 0.001). This suggests a weak or an easily reversible attachment of both LKD16 and ϕKMV to the outer membrane of *P. aeruginosa*, as observed previously with phage ϕS1 (22).

The host range of these phages was determined on a worldwide collection of 74 AFLP-typed clinical and environmental *P. aeruginosa* isolates (38). LKD16 and ϕKMV showed only minor differences in host spectrum, since 18% of the strains were infected by both phages while 2% and 5% were exclusively lysed by ϕKMV and LKD16, respectively. This host range could not be correlated to AFLP type or to differences in serotype between the tested *P. aeruginosa* strains. Despite its efficient adsorption, LKA1 displays an extremely narrow spectrum, lysing only a single strain in the library besides *P. aeruginosa* PAO1.

To explore the observed differences in phage characteristics, DNA of LKD16 and LKA1 was isolated. Restriction analysis suggested that both genomes consisted of linear double-stranded DNA, with reduced sensitivity to many type II restriction enzymes, including 6-bp cutters like BglII, BamHI, and PstI. Resistance against type II DNA restriction is common among phages (45) and can be explained by sustained evolutionary selection in numerous hosts encoding different restriction endonucleases (9).

Genome sequencing and ORF identification. The genomes of LKA1 and LKD16 were sequenced by a combination of a shotgun and a primer walking approach. For LKA1, this resulted in a final sequence of 41,593 bp that includes direct terminal repeats (DTRs) of 298 bp. The length of these DTRs was confirmed by direct sequencing with outward-directed primers, leading to a stop of the sequencing reaction at the ends of the genome. The GC content of the genome is 60.9%, which is significantly lower than the 66.6% of the *P. aeruginosa* host genome. Potential ORFs of LKA1 were identified based on gene prediction tools, tBLAST homology searches, and visual inspection of potential ORFs and their Shine-Dalgarno sequence. In this way, 56 tightly spaced ORFs were predicted, occupying 94.3% of the entire genome (Fig. 2E; see also Table S1A in the supplemental material). Although no similarity at the nucleotide level could be detected, 27 gene products show protein similarity with ϕKMV counterparts. The genome organization and gene order of ϕKMV seems largely conserved in LKA1, although some notable differences were observed, which are discussed below.

The LKD16 genome comprises 43,200 bp and has an overall GC content of 62.6%. The DTRs are 428 bp long, the longest known among T7-like phages sequenced to date and comparable to the 414-bp DTRs of ϕKMV. While no significant DNA homology to any other phage was detected in the case of LKA1, LKD16 displays an overall DNA identity of 83% with ϕKMV (Fig. 2A). Due to the extensive similarity, ORF numbering for LKD16 and ϕKMV was maintained, and newly defined or phage-unique ORFs were numbered as the preceding ϕKMV-like ORF extended with the suffix 1.

The strong DNA similarity of LKD16 and ϕKMV provided an additional tool in the sequence analysis, resulting in more thoughtful ORF predictions in both genomes. By mutual genome comparison, small putative ORFs (<150 bp) which previously fell below the threshold for gene annotation (e.g., ORFs 13.1 and 25.1) and ORFs with partially overlapping sequences (e.g., ORFs 12.1 and 46.1) are now designated as putative ORFs based on their conserved presence in both phages. It is reasonable to assume that these small conserved proteins perform a specific function in the phage infection cycle. In addition to the four newly predicted genes, ORF 41 was extended with 198 bp at the 5′ end, reducing the intergenic region between ORFs 40 and 41. Despite this major homology at the genomic level, a limited number of discrepancies do exist between LKD16 and ϕKMV. Compared to ϕKMV, two additional ORFs are defined in LKD16 (ORFs 0.1 and 17.1), ORF 9 is absent, and a 0.5-kb insert devoid of predicted ORFs is present between ORFs 3 and 4 (Fig. 2B).

Putative regulatory elements. The intergenic genome regions of LKA1 and LKD16 were searched for transcriptional regulation elements. Compared to ϕKMV, which has four potential host σ^{70} promoters in front of ORF 1, LKA1 carries three strong host promoters before ORF 1 and a fourth one in front of ORF 2. In contrast, five putative host promoters were identified within the first 1,300 bp of the LKD16 genome (Fig. 2; see also Table S2 in the supplemental material). The early ρ-independent terminator for ϕKMV (bp 5087 to 5110) seems to be present in LKA1 but is absent in LKD16. This may suggest that transcription of the LKD16 genome continues at least until terminator T1 is reached behind ORF 32. This terminator, located downstream of the major capsid protein, is present in both LKA1 and LKD16 (see Table S2) and is also found in other phages of the T7 group. In all three phages, a final terminator was defined behind the last structural protein (ORFs 48 and 56).

Analogous to ϕKMV, no conserved T7-like promoter sequences were identified in LKA1 and LKD16. Scanning the intergenic regions for conserved sequences, four putative phage promoter sites were selected for both phages (see Table S2 in the supplemental material). This number is considerably lower than the number of phage promoters predicted in other T7-like phages. Upstream AT-rich regions that play a role in modulating the efficiency of transcription initiation in T7-like phages (49) are also absent. Moreover, the consensus sequence of the predicted promoters greatly differs from other T7-like promoters and varies between ϕKMV, LKD16, and LKA1. The first putative phage promoter of LKD16 in front of ORF 4 is absent in ϕKMV, while no putative promoter sequence could be detected in the intergenic region preceding the major capsid gene of LKA1. These observations suggest slight differences in transcriptional regulation among ϕKMV, LKA1, and LKD16 and fundamental differences in regulation compared to other members of the T7 supergroup.

Mutational bias resulting from DNA replication can be exploited to gain insight in the passage of the replication fork over different parts of the genome (19, 30), elucidating the origin and terminus of replication. Analogous to SP6 (12), the number of strand-biased octamers at regular intervals in the genome sequence was determined for ϕKMV by J. G. Lawrence. In this oligomer plot, a sharp discontinuity (breakpoint) was observed around 11.5 kb, corresponding to the origin of replication (Fig. 2C). A more diffuse breakpoint was observed between 31 and 32 kb, corresponding to the replication terminus. Comparable

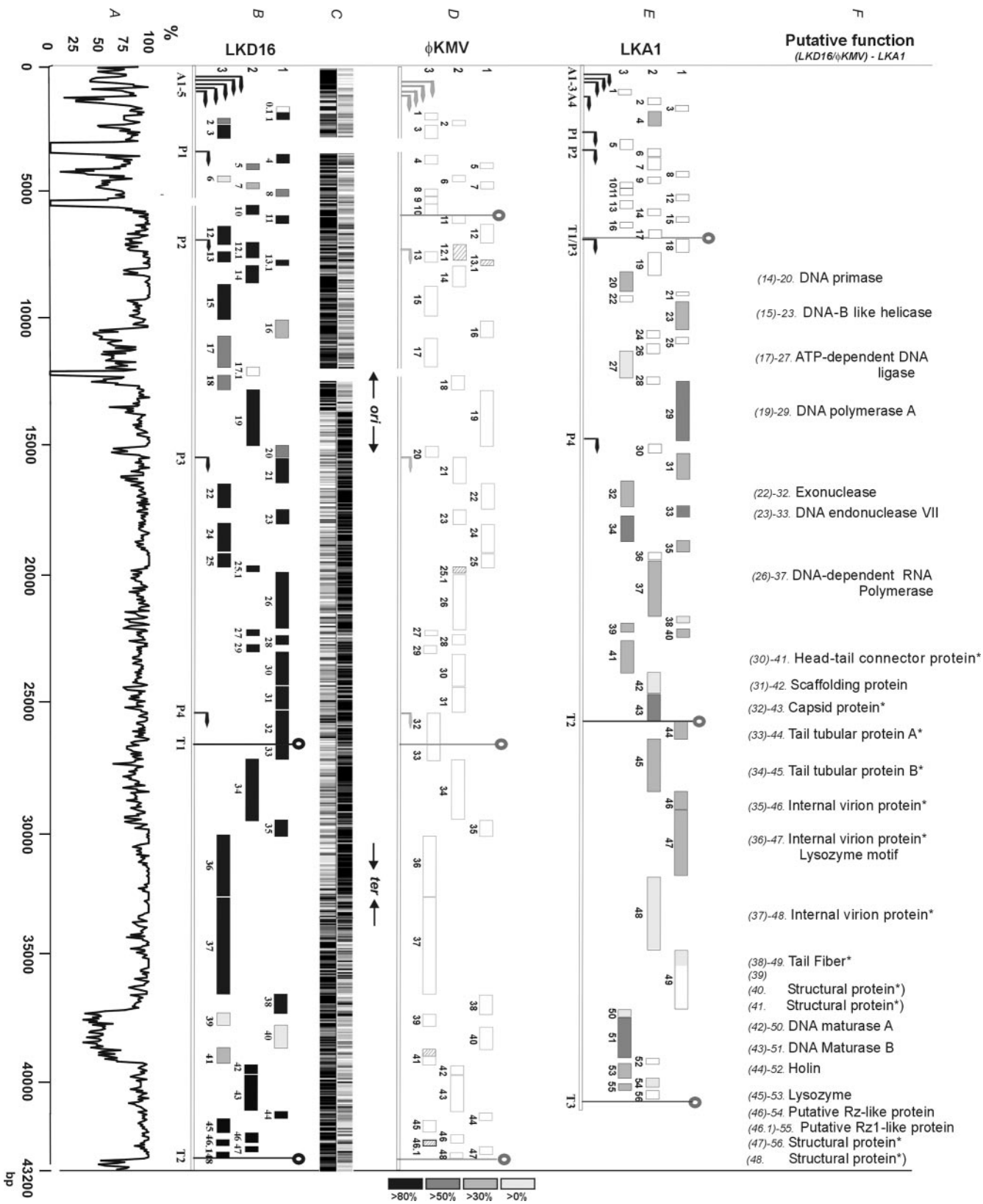

FIG. 2. Summary of the bioinformatic analysis of the ϕKMV group. (A) Pair-wise nucleotide identity of LKD16 and ϕKMV, compared ORF by ORF while using a sliding window of 50 bp. Insertions/deletions are indicated by gaps in the coding sequence. (B, D, and E) Genome comparison of LKD16, ϕKMV, and LKA1, respectively. Open reading frames and their amino acid identities with the corresponding ϕKMV proteins are indicated. Newly defined and extended ϕKMV genes are designated in hatched boxes. Putative protein functions encoded by the ϕKMV-like phages are shown in the right column (F), while experimentally confirmed structural proteins are marked by an asterisk. Putative host promoters (A), phage promoters (P), and terminators (T) are indicated. (C) Circular mutation analysis of the ϕKMV genome in order to find breakpoints where changes in strand-specific degenerate-octomeric skew are the strongest (19). The predicted origin and termination of replication are indicated by arrows.

TABLE 1. Alignment of two RNA polymerase subdomains of ϕKMV-like phages and T7

Phage	Specificity loop	Recognition loop
ϕKMV	KTEEVRVRLRAEA---VEYVTLYEAKDEL	HQEAKAA--GPAAKL
LKD16	KTEEVRVRLRAEA---VEYVTLYEAKDEL	HQEAKAA--GPAAKL
LKA1	DFVEHRVKIRSCG---ITDIVVREDLDQT	VVETKAR--GPGAAL
T7	KPIQTRLNLMFLGQFRLQPTINTNKDSEI	WFEEVKAKRGKRPTA

to SP6, this analysis suggests a bidirectional replication originating within the coding sequence of the DNA polymerase (ORF 19) and terminating in the internal virion protein (ORF 37). Visual inspection of this region did not reveal an AT-rich primase binding site, as is present in T7.

Early genes and DNA replication genes. Comparing the three phage genomes and considering putative gene functions, two functional genomic regions can be delineated. The first genomic region ends after the RNA polymerase gene and encompasses genes for host conversion (early genes) and DNA replication, while the second (late) region comprises genes coding for structural and lysis proteins. An interesting feature is the diversity among the early phage genes. The early region of LKA1 has strongly diverged and encodes 18 small proteins with no similarity to other gene products (gp) in the GenBank database. The only exception is gp4, which displays minor similarity to gp3 of ϕKMV and gp70 of *Pseudomonas* phage PaP3 (NC_004466). In contrast, the early region of LKD16 is closely related to ϕKMV. Although DNA homology is lower in this genome region (58%), all corresponding ϕKMV ORFs are present (except for ORF 9) and only one ORF (0.1) is unique for LKD16.

Gene order among the DNA replication genes is conserved in the three phages, except for ORF 16 of ϕKMV, which is replaced by three smaller ORFs in LKA1 (Fig. 2E). Although protein similarity to the T7-like phages is only found in the DNA ligase (28% identity), gene products encoded within this region seem functionally consistent with the corresponding proteins of the T7 sensu stricto phages. However, major similarity is found with DNA replication genes of *Xanthomonas oryzae* phage Xp10 (54) and with a *Siphoviridae*-like prophage within the genome of *Burkholderia pseudomallei* 1710b (NC_007434). Remarkably, the *Siphoviridae* Xp10 also encodes a T7-like single-subunit RNA polymerase downstream of its DNA replication genes, emphasizing once more the truly mosaic nature of bacteriophages.

Phage RNA polymerase. In contrast to other T7-like phages but similar to ϕKMV, the predicted RNA polymerases of LKD16 and LKA1 are not located among the early genes but at the end of the DNA replication region. The LKA1 and LKD16 RNA polymerases are definitely related to T7 (BlastP expected values of e^{-65} and e^{-68}, respectively) with broad conservation of the subdomains and of the essential catalytic residues Tyr639, Lys631, Asp537, and Asp812 (10, 11). However, no homology can be detected in their recognition loop (amino acids [aa] 93 to 101) and specificity loop (aa 739 to 770), which interact with nucleotides −17 to −13 and −7 to −11 of the T7-like phage promoters, respectively (10, 11). These two regions are perfectly conserved between ϕKMV and LKD16 (Table 1), which is in agreement with the similarity of their predicted promoter sequences (see Table S2 in the supplemental material). The LKA1 RNA polymerase shares some similarity to ϕKMV in the recognition loop, but the promoter specificity loop has strongly diverged. These observations explain the differences in promoter specificity between LKA1, LKD16, and T7.

Phage structural proteins. Using MS approaches, 12 predicted ORFs were previously confirmed as part of the ϕKMV phage particle (27). In contrast to the ϕKMV particle analysis, which was restricted to visual protein bands, the entire lane of a one-dimensional sodium dodecyl sulfate-polyacrylamide gel electrophoresis gel containing structural LKA1 and LKD16 proteins was cut into slices for subsequent trypsin digestion and ESI-MS/MS analysis. Consequently, less abundant proteins or peptides migrating between visible bands were not overlooked. Table 2 summarizes the experimentally confirmed structural proteins of both phages, displaying the number of significant sequence-identified nonsibling peptides and the resulting sequence coverage of the entire protein. As expected for LKD16, all the ORFs corresponding to the identified particle proteins of ϕKMV (27) were also found in LKD16. In addition, gp41 of LKD16 was identified as a structural protein. Analysis of the MS data pointed out that the two most significantly identified peptides of gp41 are located at the N terminal

TABLE 2. Identification of the structural proteins of LKA1 and LKD16

Putative function	LKA1				LKD16				Previous identification in ϕKMV[a]
	Gene no.	Mol. mass (kDa)	No. of peptides	Sequence coverage (%)	Gene no.	Mol. mass (kDa)	No. of peptides	Sequence coverage (%)	
Unknown	40	8.9	5	88.9	29	10.5	4	48.9	+
Connector	41	56.6	16	51.9	30	56.1	11	29.1	+
Capsid	43	36.7	23	83.2	32	37.7	21	64.6	+
Tail protein A	44	23.4	2	21.4	33	21.2	2	18.2	+
Tail protein B	45	84.4	17	31.2	34	92.0	12	21.6	+
Internal virion	46	21.6	2	16.1	35	18.8	5	30.9	−
Internal virion	47	93.9	50	69.3	36	98.2	19	37.2	+
Internal virion	48	108.0	32	50.1	37	143.8	17	18.7	+
Tail fiber	49	80.4	16	33.6	38	28.5	6	32.2	+
Adsorption					40	31.8	5	27.5	+
Adsorption					41	22.7	4	35.8	−
Unknown	56	10.7	2	42.4	47	10.5	7	86.5	+
Unknown					48	6.8	2	42.2	+

[a] As stated in reference 27.

TABLE 3. Features of the lysis-related genes of LKD16, ϕKMV, and LKA1

Phage(s)	Gene product	N-terminal sequence[a]			Signal sequence probability[a]
LKD16 and ϕKMV	gp45	VNKPLR	GAALAAALAGLVAL	EGSETTA	0.99
	gp46	MPRT	IVAILVLAVVALG	ASYGFVQ SYRALG	0.99
	gp46.1	VPWTRT	ARGLTGLCLLLS	LTACAT APAPA	1.00
LKA1	gp53	MRKFK	ATLTAAALAL	GLGTGV VYNAAEFI	0.99
	gp54	MRLT	VALILALVVAV	GAGLYAA QKAWQYHR	0.99
	gp55	MKNLL	GGMLLCLLPFVAS	CASSSSA EPVRC	1.00

[a] Signal sequences were predicted using SignalP, showing for each protein the signal sequence probability. The first, second, and third segments are the N, H, and C domains, respectively.

of the gene product, which was previously not defined as part of the coding region of ORF 41 in ϕKMV (Fig. 2D; see also Table S1A in the supplemental material). This observation supports the revised annotation of this ORF, expanding the 5′ end of the gene with 198 bp. The smallest putative internal virion protein of LKD16 (gp35) was also confirmed as a structural protein. In this way, all predicted proteins in the structural genome region of LKD16 were experimentally identified, except for the scaffolding protein and gp39, which may not be part of the mature phage particle.

One of the most intriguing differences between LKD16 and ϕKMV is located in the tail fiber section. In sharp contrast with the other structural proteins that are nearly perfectly conserved, gp39, -40, and -41 show only 50, 25, and 50% conservation, respectively (Fig. 2B). Similarity searches yielded no putative function for these genes, but gp40 and gp41 were shown to be part of the LKD16 phage particle, presumably playing a role in phage adhesion to the host (see Discussion).

The structural region of LKA1 shares an overall 30 to 50% protein similarity to ϕKMV and LKD16, encompassing proteins encoded between ORF 40 and ORF 49 and including ORF 56 (Table 2 and Fig. 2E). Compared to ϕKMV and LKD16, deletions are present in genes encoding the scaffolding protein (180 bp) and the largest internal virion protein (999 bp). Even more remarkable is the apparent replacement of ORFs 38, 39, 40, and 41 by a single ORF in LKA1 (ORF 49). Blast analyses on gp49 revealed similarity at the N terminal to several T7-like tail fibers, probably attaching this N-terminal end of the protein to the phage virion. However, the C-terminal part of gp49 displays major similarity (BlastP expected value of e^{-68}) to gp27 of the temperate *P. aeruginosa* phage D3. The function of gp27 of D3 is not known (24), but its gene is located just upstream a serotype-converting module (34). Since this C-terminal part of gp49 was picked up in the MS analysis, a particle-associated role for gp27 in D3 can be proposed. The major homology between D3-gp27 and the putative tail fiber of LKA1 is located at the N terminal of gp27. The C terminal of gp49 has further differentiated, and iterative psi-BLAST searches point to a minor similarity with fungal β-1-3 glucanases. The putative role of this protein in the binding and/or (partial) degradation of the host cell wall is currently under investigation.

Lysis mechanism. Most phages use a combination of a holin and an endolysin to release newly formed phage particles. These ORFs (44 and 45, respectively) are nearly perfectly conserved between LKD16 and ϕKMV. Analysis of the N-terminal sequence of the endolysins (gp45) of both phages reveals the presence of an identical signal sequence (Table 3), suggesting a signal-arrest and release mechanism, which was recently demonstrated for ϕKMV (R. Lavigne et al., unpublished data). In this phage release mechanism, first described for coliphage P1, the N-terminal signal sequence of the lysin mediates Sec transport to the periplasm (52). In gp45 of ϕKMV and LKD16, however, the C-terminal domain of the signal sequence, responsible for endopeptidase cleavage, is absent. The lysin molecules are probably released upon destabilization of the inner membrane by a class II holin (51). Furthermore, many phages encode internally overlapping Rz/Rz1 proteins immediately downstream of the endolysin to improve bacterial lysis when the outer membrane is stabilized by divalent cations (17, 21). It is suggested that these gene products form a complex after translocation to the periplasm and destabilize the cell wall by cleavage of the oligopeptide links between the murein and the outer membrane protein Lpp (53). In-depth comparative analysis of ϕKMV and LKD16 suggests that ORF 46 contains in both phages a conserved out-of-frame internal ORF 46.1. Both ORFs have a clear ribosomal binding site, and the corresponding proteins contain a true periplasmic signal sequence at the N terminal, an essential feature for Rz/Rz-like proteins (Table 3).

The lysis cassette of LKA1 carries the same backbone structure. Despite only limited protein similarity, a signal peptide is predicted at the N terminal of gp53, -54, and -55, which presumably encode the endolysin and the Rz/Rz1-like proteins, respectively (Table 3). Moreover, two hydrophobic domains are present in gp52, suggesting its function as a class II holin. In contrast to ϕKMV and LKD16, a potential dual translational start motif is predicted in the coding sequence of gp52. In this motif (*M*TK*M*), two methionine residues are separated by a positively charged amino acid, leading to two proteins of slightly different size (68 and 65 aa). Analogous to the class II holin proteins of phage 21 (5), a fine-tuned regulation of host lysis by a shorter holin effector and a longer holin inhibitor is proposed.

DISCUSSION

Sequencing of closely related phages. The high degree of homology between LKD16 and ϕKMV provided a unique opportunity for comparative analysis of these *P. aeruginosa* phages. Although sequencing of closely related phages may cause a certain bias towards "model" phages in the genomic

databases, the determination of these genomes can lead to further insight into their coding sequences, genomic organization, and regulation. Especially small potential ORFs (<150 bp) are usually ignored in the annotation of phage genomes and might be overlooked in later stages of phage research. The encoded gene products, however, may have important biological functions. A good example of such an active polypeptide is the phage T4-encoded Stp protein, which is only 26 amino acids long and activates the host PrrC lysyl-tRNA endonuclease (37). The comparative analysis of both phages resulted in a reannotation of the ϕKMV genome, defining four new ORFs and extending the 5′ end of ORF 41 with 198 bp. Furthermore, putative Rz/Rz1-like proteins were annotated in all three genomes. The usefulness of this comparative analysis was experimentally confirmed by the identification of the newly defined N terminal of gp41 using ESI-MS/MS. This MS analysis of phage proteins proved to be a comprehensive technique in the verification of predicted proteins, experimentally confirming 13 (24%) and 10 (18%) gene products as being part of the LKD16 and LKA1 particles, respectively.

Comparison of ϕKMV-like phages. Phage LKD16 appears to be a very close relative of ϕKMV, showing a conserved genome organization and major similarity in 96% of its encoded proteins. Despite similar adsorption kinetics, notable differences in phenotypic properties do occur. Most likely, the insertions and deletions within the early region account for the intriguing differences in burst size and latent period, while small variations observed in host range are probably caused by altered tail fiber proteins. Compared to LKD16, ϕKMV lacks the first putative phage promoter and carries a terminator between ORFs 10 and 11 (26).

Genome analysis clearly showed that LKA1 is more distantly related to LKD16 and ϕKMV, displaying protein similarity to these phages in 48% of its predicted gene products. Like LKD16, the main variations are located within the early genes and the tail fiber genes, but these regions are much more diverged in case of LKA1. These discrepancies can be associated with differences in adsorption and host range, since LKD16 and ϕKMV both carry four genes with a possible role in phage adsorption, while LKA1 carries only one predicted tail fiber gene (ORF 49). While the N terminal of gp49 probably connects the fiber to the virion particle, the C terminal might contain enzymatic activity, which would be consistent with tail structures found in other phages like K1F and PK1E (46). Adsorption and infection of ϕKMV and LKD16 might also be influenced by the two small proteins (gp47 and gp48) at the right end of the genome, which have one counterpart (gp56) in LKA1. These proteins downstream of the lysis cassette are not found in the T7-like phages but are experimentally confirmed in the phages of the SP6 subgroup (45).

Bioinformatic analysis suggests that DNA replication of ϕKMV occurs through a bidirectional mechanism, with the *ori* located within the gene encoding the DNA polymerase. The position of the replication start is conserved in ϕKMV, SP6, and lambdoid phages (12). It is reasonable to assume that the DNA polymerase gene and its target *ori* coevolved and remained linked in a mosaic-based evolution. However, this is not a common feature among all T7-like phages (J. G. Lawrence, personal communication).

Transcriptional control seems to be conserved among the ϕKMV-like phages and probably differs greatly from T7 sensu stricto phages. This can be deduced from the genomic localization of the phage RNA polymerase, downstream of the DNA replication genes, and the absence of conserved T7-like phage promoter sequences. This inevitably implies a higher dependency to the host RNA polymerase for transcription of early phage genes, illustrated by relatively high numbers of host promoters.

The ϕKMV subgroup within the T7 supergroup. The closely related lytic phages like ϕKMV and LKD16 (and to a lesser extent LKA1) were isolated from water samples from different countries (Russia and Belgium, respectively). Although little is known about phage biodiversity and biogeography, local viral diversity seems to be high, whereas global diversity is relatively low because viruses are moving between environments (8). As seen with T7, T3, ϕA1122, and ϕYe03-12, phages that were isolated over time, in different habitats and infecting different hosts, were shown to have up to 89% DNA homology (15, 35, 36). This widespread nature is confirmed by findings of well-conserved T7-like DNA polymerases in phages isolated from extremely different global ecosystems (7). By moving between environments, phages facilitate horizontal gene transfer, as exemplified by the similarity between the tail fiber gene of LKA1 and gp27 of the temperate phage D3. Based on their overall genome organization, LKA1, LKD16, and ϕKMV clearly belong to the T7 supergroup within the *Podoviridae*. Compared with T7 sensu stricto phages, however, they have probably evolved separately from a no-longer-extant common ancestor, as illustrated by the diverged localization of the RNA polymerase and the predicted phage promoter sequences. Therefore, ϕKMV, LKD16, and LKA1 can be considered a separate ϕKMV subgroup of widespread and common phages infecting *Pseudomonas aeruginosa*. Additional evidence of the wide environmental distribution of this type of lytic phages was recently provided by the isolation of several phages from various Russian environmental samples, which were annotated as ϕKMV-like phages based on Southern hybridization experiments (9). Future phage isolations towards nonlaboratory strains of *P. aeruginosa* and analysis of their genomes and lytic behavior will lead to a more comprehensive view of the prevalence and antimicrobial potential of virulent *P. aeruginosa* phages.

ACKNOWLEDGMENTS

We are very grateful to Jeffrey Lawrence (Department of Biological Sciences, University of Pittsburgh) for the skew analysis on the ϕKMV genome and to Jean-Paul Pirnay (Epidemiology and Bio-statistics Division, Department of Well-being, Queen Astrid Military Hospital, Belgium) for the clinical *P. aeruginosa* strains.

Pieter-Jan Ceyssens holds a predoctoral fellowship of the Instituut voor de aanmoediging van Innovatie door Wetenschap en Technologie in Vlaanderen (Belgium). Kirsten Hertveldt holds a postdoctoral fellowship of the Fonds voor Wetenschappelijk Onderzoek-Vlaanderen (FWO-Vlaanderen, Belgium). This work was financially supported by the research council of the KULeuven grants OT/04/30 and OT/05/47 and the Flemish FWO research grant G.0308.05.

REFERENCES

1. **Adams, M. H.** 1959. Bacteriophages, p. 14–15. Interscience Publishers, Inc., New York, N.Y.
2. **Altschul, S. F., W. Gish, W. Miller, E. W. Myers, and D. J. Lipman.** 1990. Basic local alignment search tool. J. Mol. Biol. **215:**403–410.
3. **Altschul, S. F., T. L. Madden, A. A. Schaffer, J. Zhang, Z. Zhang, W. Miller,**

and D. J. Lipman. 1997. Gapped BLAST and PSI-BLAST: a new generation of protein database search programs. Nucleic Acids Res. **25:**3389–3402.
4. **Bailey, T. L., and M. Gribskov.** 1998. Combining evidence using p-values: application to sequence homology searches. Bioinformatics **14:**48–54.
5. **Barenboim, M., C. Y. Chang, F. dib Hajj, and R. Young.** 1999. Characterization of the dual start motif of a class II holin gene. Mol. Microbiol. **32:**715–727.
6. **Bendtsen, J. D, H. Nielsen, G. von Heijne, and S. Brunak.** 2004. Improved prediction of signal peptides: SignalP 3.0. J. Mol. Biol. **340:**783–795.
7. **Breitbart, M., J. H. Miyake, and F. Rohwer.** 2004. Global distribution of nearly identical phage-encoded DNA sequences. FEMS Microbiol. Lett. **236:**249–256.
8. **Breitbart, M., and F. Rohwer.** 2005. Here a virus, there a virus, everywhere the same virus? Trends Microbiol. **13:**278–284.
9. **Burkal'tseva, M. V., E. A. Pleteneva, O. V. Shaburova, V. A. Kadykov, and V. N. Krylov.** 2006. Genome conservatism of ϕKMV-like bacteriophages (T7 supergroup) active against *Pseudomonas aeruginosa*. Genetika **42:**33–38.
10. **Cheetham, G. M., and T. A. Steitz.** 2000. Insights into transcription: structure and function of single-subunit DNA-dependent RNA polymerases. Curr. Opin. Struct. Biol. **10:**117–123.
11. **Cheetham, G. M., and T. A. Steitz.** 1999. Structure of a transcribing T7 RNA polymerase initiation complex. Science **286:**2305–2309.
12. **Dobbins, A. T., M. George, Jr., D. A. Basham, M. E. Ford, J. M. Houtz, M. L. Pedulla, J. G. Lawrence, G. F. Hatfull, and R. W. Hendrix.** 2004. Complete genomic sequence of the virulent *Salmonella* bacteriophage SP6. J. Bacteriol. **186:**1933–1944.
13. **Dunn, J. J., and F. W. Studier.** 1983. Complete nucleotide sequence of bacteriophage T7 DNA and the locations of T7 genetic elements. J. Mol. Biol. **166:**477–535.
14. **Ganguly, T., P. Chen, R. Teetsel, L. P. Zhang, E. Papaioannou, and J. Cianciarlo.** 2005. High-throughput sequencing of high copy number plasmids from bacterial cultures by heat lysis. BioTechniques **39:**304–308.
15. **Garcia, E., L. M. Elliott, E. Ramanculov, P. S. Chain, M. C. Chu, and I. J. Molineux.** 2003. The genome sequence of *Yersinia pestis* bacteriophage ϕA1122 reveals an intimate history with the coliphage T3 and T7 genomes. J. Bacteriol. **185:**5248–5262.
16. **Gill, J. J., A. M. Svircev, R. Smith, and A. J. Castle.** 2003. Bacteriophages of *Erwinia amylovora*. Appl. Environ. Microbiol. **69:**2133–2138.
17. **Hanych, B., S. Kedzierska, B. Walderich, B. Uznanski, and A. Taylor.** 1993. Expression of the Rz gene and the overlapping Rz1 reading frame present at the right end of the bacteriophage lambda genome. Gene **129:**1–8.
18. **Hardies, S. C., A. M. Comeau, P. Serwer, and C. A. Suttle.** 2003. The complete sequence of marine bacteriophage VpV262 infecting *Vibrio Parahaemolyticus* indicates that an ancestral component of a T7 viral supergroup is widespread in the marine environment. Virology **310:**359–371.
19. **Hendrickson, H., and J. G. Lawrence.** 2006. Selection for chromosome architecture in bacteria. J. Mol. Evol. **62:**615–629.
20. **Imberechts, H., P. Wild, G. Charlier, H. De Greve, P. Lintermans, and P. Pohl.** 1996. Characterization of F18 fimbrial genes fedE and fedF involved in adhesion and length of enterotoxemic *Escherichia coli* strain 107/86. Microb. Pathog. **21:**183–192.
21. **Kedzierska, S., A. Wawrzynow, and A. Taylor.** 1996. The Rz1 gene product of bacteriophage lambda is a lipoprotein localized in the outer membrane of *Escherichia coli*. Gene **168:**1–8.
22. **Kelln, R. A., and R. A. Warren.** 1971. Isolation and properties of a bacteriophage lytic for a wide range of pseudomonads. Can. J. Microbiol. **17:**677–682.
23. **Kovalyova, I. V., and A. M. Kropinski.** 2003. The complete genomic sequence of lytic bacteriophage gh-1 infecting *Pseudomonas putida*-evidence for close relationship to the T7 group. Virology **311:**305–315.
24. **Kropinski, A. M.** 2000. Sequence of the genome of the temperate, serotype-converting, *Pseudomonas aeruginosa* bacteriophage D3. J. Bacteriol. **182:**6066–6074.
25. **Lavigne, R., Y. Briers, K. Hertveldt, J. Robben, and G. Volckaert.** 2004. Identification and characterization of a highly thermostable bacteriophage lysozyme. Cell Mol. Life Sci. **61:**2753–2759.
26. **Lavigne, R., M. V. Burkal'tseva, J. Robben, N. N. Sykilinda, L. P. Kurochkina, B. Grymonprez, B. Jonckx, V. N. Krylov, V. V. Mesyanzhinov, and G. Volckaert.** 2003. The genome of bacteriophage ϕKMV, a T7-like virus infecting *Pseudomonas aeruginosa*. Virology **312:**49–59.
27. **Lavigne, R., J. P. Noben, K. Hertveldt, P. J. Ceyssens, Y. Briers, D. Dumont, B. Roucourt, V. N. Krylov, V. V. Mesyanzhinov, J. Robben, and G. Volckaert.** 2006. The structural proteome of *Pseudomonas aeruginosa* bacteriophage ϕKMV. Microbiology **152:**529–534.
28. **Lavigne, R., W. D. Sun, and G. Volckaert.** 2004. PHIRE, a deterministic approach to reveal regulatory elements in bacteriophage genomes. Bioinformatics **20:**629–635.
29. **Lawrence, J. G., G. F. Hatfull, and R. W. Hendrix.** 2002. Imbroglios of viral taxonomy: genetic exchange and failings of phenetic approaches. J. Bacteriol. **184:**4891–4905.
30. **Lobry, J. R.** 1996. Asymmetric substitution patterns in the two DNA strands of bacteria. Mol. Biol. Evol. **13:**660–665.
31. **Lukashin, A. V., and M. Borodovsky.** 1998. GeneMark.hmm: new solutions for gene finding. Nucleic Acids Res. **26:**1107–1115.
32. **Moller, S., M. D. Croning, and R. Apweiler.** 2001. Evaluation of methods for the prediction of membrane spanning regions. Bioinformatics **17:**646–653.
33. **Nelson, K. E., C. Weinel, I. T. Paulsen, R. J. Dodson, H. Hilbert, V. A. Martins dos Santos, D. E. Fouts, S. R. Gill, M. Pop, M. Holmes, L. Brinkac, M. Beanan, R. T. DeBoy, S. Daugherty, J. Kolonay, R. Madupu, W. Nelson, O. White, J. Peterson, H. Khouri, I. Hance, P. Chris Lee, E. Holtzapple, D. Scanlan, K. Tran, A. Moazzez, T. Utterback, M. Rizzo, K. Lee, D. Kosack, D. Moestl, H. Wedler, J. Lauber, D. Stjepandic, J. Hoheisel, M. Straetz, S. Heim, C. Kiewitz, J. A. Eisen, K. N. Timmis, A. Dusterhoft, B. Tummler, and C. M. Fraser.** 2002. Complete genome sequence and comparative analysis of the metabolically versatile *Pseudomonas putida* KT2440. Environ. Microbiol. **4:**799–808.
34. **Newton, G. J., C. Daniels, L. L. Burrows, A. M. Kropinski, A. J. Clarke, and J. S. Lam.** 2001. Three-component-mediated serotype conversion in *Pseudomonas aeruginosa* by bacteriophage D3. Mol. Microbiol. **39:**1237–1247.
35. **Pajunen, M. I., M. R. Elizondo, M. Skurnik, J. Kieleczawa, and I. J. Molineux.** 2002. Complete nucleotide sequence and likely recombinatorial origin of bacteriophage T3. J. Mol. Biol. **319:**1115–1132.
36. **Pajunen, M., S. Kiljunen, and M. Skurnik.** 2000. Bacteriophage ϕYeO3-12, specific for *Yersinia enterocolitica* serotype O:3, is related to coliphages T3 and T7. J. Bacteriol. **182:**5114–5120.
37. **Penner, M., I. Morad, L. Snyder, and G. Kaufmann.** 1995. Phage T4-coded Stp: double-edged effector of coupled DNA and tRNA-restriction systems. J. Mol. Biol. **249:**857–868.
38. **Pirnay, J. P., D. De Vos, C. Cochez, F. Bilocq, A. Vanderkelen, M. Zizi, B. Ghysels, and P. Cornelis.** 2002. *Pseudomonas aeruginosa* displays an epidemic population structure. Environ. Microbiol. **4:**898–911.
39. **Reese, M. G.** 2001. Application of a time-delay neural network to promoter annotation in the *Drosophila melanogaster* genome. Comput. Chem. **26:**51–56.
40. **Rice, P., I. Longden, and A. Bleasby.** 2000. EMBOSS: the European molecular biology open software suite. Trends Genet. **16:**276–277.
41. **Rohwer, F., A. Segall, G. Steward, V. Seguritan, M. Breitbart, F. Wolven, and F. Azam.** 2000. The complete genomic sequence of the marine phage Roseophage SIO1 shares homology with nonmarine phages. Limnol. Oceanogr. **45:**408–418.
42. **Rohwer, F., and R. Edwards.** 2002. The Phage Proteomic Tree: a genome-based taxonomy for phage. J. Bacteriol. **184:**4529–4535.
43. **Sambrook, J., and D. W. Russell.** 2001. Molecular cloning: a laboratory manual, 3rd ed., vol. 1, p. 2.56–2.58. Cold Spring Harbor Laboratory Press, Cold Spring Harbor, N.Y.
44. **Scholl, D., S. Adhya, and C. R. Merril.** 2002. Bacteriophage SP6 is closely related to phages K1-5, K5, and K1E but encodes a tail protein very similar to that of the distantly related P22. J. Bacteriol. **184:**2833–2836.
45. **Scholl, D., J. Kieleczawa, P. Kemp, J. Rush, C. C. Richardson, C. R. Merril, S. Adhya, and I. J. Molineux.** 2004. Genomic analysis of bacteriophages SP6 and K1-5, an estranged subgroup of the T7 supergroup. J. Mol. Biol. **335:**1151–1171.
46. **Scholl, D., and C. R. Merril.** 2005. The genome of bacteriophage K1F, a T7-like phage that has acquired the ability to replicate on K1 strains of *Escherichia coli*. J. Bacteriol. **187:**8499–8503.
47. **Shevchenko, A., M. Wilm, O. Vorm, O. N. Jensen, A. V. Podtelejnikov, G. Neubauer, and M. Mann.** 1996. A strategy for identifying gel-separated proteins in sequence databases by MS alone. Biochem. Soc. Trans. **24:**893–896.
48. **Stone, R.** 2002. Bacteriophage therapy. Stalin's forgotten cure. Science **298:**728–731.
49. **Tang, G. Q., R. P. Bandwar, and S. S. Patel.** 2005. Extended upstream A-T sequence increases T7 promoter strength. J. Biol. Chem. **280:**40707–40713.
50. **Taylor, J. A., and R. S. Johnson.** 1997. Sequence database searches via *de novo* peptide sequencing by tandem mass spectrometry. Rapid Commun. Mass Spectrom. **11:**1067–1075.
51. **Xu, M., A. Arulandu, D. K Struck, S. Swanson, J. C. Sacchettini, and R. Young.** 2005. Disulfide isomerization after membrane release of its SAR domain activates P1 lysozyme. Science **307:**113–117.
52. **Xu, M., D. K. Struck, J. Deaton, I. N. Wang, and R. Young.** 2004. A signal-release sequence export and control of the phage P1 endolysin. Proc. Natl. Acad. Sci. USA **101:**6415–6420.
53. **Young, R., I. Wang, and W. D. Roof.** 2000. Phages will out: strategies of host cell lysis. Trends Microbiol. **8:**120–128.
54. **Yuzenkova, J., S. Nechaev, J. Berlin, D. Rogulja, K. Kuznedelov, R. Inman, A. Mushegian, and K. Severinov.** 2003. Genome of *Xanthomonas oryzae* bacteriophage Xp10: an odd T-odd phage. J. Mol. Biol. **330:**735–748.
55. **Zuker, M.** 1989. On finding all suboptimal foldings of an RNA molecule. Science **244:**48–52.